PCCP

PAPER

View Article Online
View Journal | View Issue

Cite this: *Phys. Chem. Chem. Phys.*, 2019, **21**, 7847

C_nTAB/polystyrene sulfonate mixtures at air–water interfaces: effects of alkyl chain length on surface activity and charging state†

Felix Schulze-Zachau and Björn Braunschweig *

Binding and phase behavior of oppositely charged polyelectrolytes and surfactants with different chain lengths were studied in aqueous bulk solutions and at air–water interfaces. In particular, we have investigated the polyanion poly(sodium 4-styrenesulfonate) (NaPSS) and the cationic surfactants dodecyltrimethylammonium bromide (C_{12}TAB), tetradecyltrimethylammonium bromide (C_{14}TAB) and cetyltrimethylammonium bromide (C_{16}TAB). In order to reveal the surfactant/polyelectrolyte binding, aggregation and phase separation of the mixtures, we have varied the NaPSS concentration systematically and have kept the surfactant concentration fixed at 1/6 of the respective critical micelle concentration. Information on the behavior in the bulk solution was gained by electrophoretic mobility and turbidity measurements, while the surface properties were studied using surface tension measurements and vibrational sum-frequency generation (SFG). This has enabled us to relate bulk to interfacial properties with respect to the charging state and the surfactants' binding efficiency. We found that the latter two are strongly dependent on the alkyl chain length of the surfactant and that binding is much more efficient as the alkyl chain length of the surfactant increases. This also results in a different phase behavior as shown by turbidity measurements of the bulk solutions. Charge neutral aggregates that are forming in the bulk adsorb onto the air–water interface – an effect that is likely caused by the increased hydrophobicity of C_nTAB/PSS complexes. This conclusion is corroborated by SFG spectroscopy, where we observe a decrease in the intensity of O–H stretching bands, which is indicative of a decrease in surface charging and the formation of interfaces with negligible net charge. Particularly at mixing ratios that are in the equilibrium two-phase region, we observe weak O–H intensities and thus surface charging.

Received 25th February 2019,
Accepted 5th March 2019

DOI: 10.1039/c9cp01107b

rsc.li/pccp

1. Introduction

The unique physicochemical properties of polyelectrolyte/surfactant (P/S) mixtures both in bulk solutions and at aqueous interfaces make them interesting candidates for many applications and have attracted considerable interest.[1–4] Applications range from industrial usage such as in mineral processing and oil recovery to cosmetic and pharmaceutical formulations, *e.g.* for hair care products or drug delivery.[5–12] In most cases, pure polyelectrolytes do not show a significant surface activity, which is why surfactants are often added to influence the interface properties of polyelectrolytes in a targeted way. In this respect, mixtures of oppositely charged polyelectrolytes and surfactants are of special interest.[1,8,13–19]

In applications of soft matter materials, polyelectrolytes are used as flocculants and stabilizers due to electrostatic and entropic interactions, which makes them ideal candidates also for stabilization of colloidal solutions and thin liquid films.[20] Therefore, foams, emulsions and thin liquid films of polyelectrolytes[21,22] and polyelectrolyte/surfactant mixtures[23–33] have been studied previously. Varga and Campbell provide a general description of the physical behavior of oppositely charged polyelectrolyte/surfactant mixtures for both polycation/anionic and polyanion/cationic surfactants.[3] The general behavior of the latter mixtures is described by the slow precipitation of aggregates in the equilibrium two-phase region, which is characterized by a lack of colloidal stability at bulk compositions close to charge neutralization. In this equilibrium two-phase region, aggregation and sedimentation occur and leave a depleted supernatant after a sufficient waiting time. Consequently, this leads also to a depletion of surface-active material and can cause a so-called "cliff edge peak" in the surface tension isotherm after a sufficient equilibration time.[34] Differences are observed in the binding efficiency of surfactants to polyelectrolytes and in the ageing behavior of the different S/P mixtures. Ábrahám *et al.* observed similar effects for mixtures of NaPSS with DTAB and analyzed the effect of ionic strength on the aggregation and changes in the surface tension isotherms.[35] They developed a model for

Institute of Physical Chemistry and Center for Soft Nanoscience, Westfälische Wilhelms-Universität Münster, Corrensstraße 28/30, 48149 Münster, Germany. E-mail: braunschweig@uni-muenster.de

† Electronic supplementary information (ESI) available. See DOI: 10.1039/c9cp01107b

the prediction of the surface tension of such mixtures, which is based on the surface tension of the pure surfactant and additional bulk measurements.[36] The same system was investigated earlier by Noskov *et al.*[37] who reported that the dynamic surface elasticity is highly dependent on the S/P mixing ratio and their molecular interactions. Noskov *et al.* also provided an overview of the surface viscoelasticity of S/P mixtures for a range of different systems.[38]

As an experimental method to study polyelectrolytes at fluid interfaces, neutron reflectometry (NR) has been demonstrated as a powerful tool, particularly for investigations of their surface properties. Consequently, NR was often applied to study polyelectrolyte/surfactant mixtures at air–water interfaces.[16,39–44] In fact, the effect of surfactant chain length on the thickness of NaPSS/C_nTAB layers adsorbed onto the air–water interface has been studied using NR by Taylor *et al.*[14] However, they varied the surfactant concentration (as opposed to the polyelectrolyte concentration in our work) and did not report the differences in the binding behavior and the surface charge of polyelectrolyte–surfactant complexes at the air–water interface.

In our previous work, we have investigated in detail the interactions between poly(sodium 4-styrenesulfonate) (NaPSS) and cetyltrimethylammonium bromide (C_{16}TAB).[4] The polyelectrolyte used was shown to have an inherent surface activity if the concentration is high enough.[45] For NaPSS/C_{16}TAB mixtures, charge neutral complexes are observed close to equimolar mixing ratios of the two components. At this concentration, we also observed a minimum in surface tension and charge neutral complexes at the interface, which was evidenced by vibrational sum-frequency generation (SFG) spectroscopy. At a threshold concentration that is slightly above this point of zero net charge, we observed a depletion of material from the interface according to surface tension and ellipsometry measurements, similar to what Campbell and co-workers have seen for mixtures of poly(acrylamidomethylpropanesulfonate) sodium salts (PAMPS) with C_{14}TAB.[46] However, it is likely that with a change in the surfactant–polyelectrolyte interactions, *e.g.* by variations of the surfactant alkyl chain length, differences in the binding between surfactants and polyelectrolytes can occur. For that reason, we present in this work a first detailed study on the effects of surfactant alkyl chain lengths on equilibrium and non-equilibrium properties of C_nTAB/NaPSS mixtures at air–water interfaces as a function of mixing ratio and alkyl chain length with n = 12, 14 and 16. Using a multi-technique approach, our study provides new information on the physical chemistry of S/P mixtures in the bulk solution and at air–water interfaces.

2. Materials and methods

2.1 Materials

Poly(sodium 4-styrenesulfonate) with a molecular weight of 70 kDa (PDI < 1.2, batch no. BCBP3081V), dodecyltrimethylammonium bromide (C_{12}TAB, ≥99%), tetradecyltrimethylammonium bromide (C_{14}TAB, ≥99%) and cetyltrimethylammonium bromide (C_{16}TAB, ≥99%) were purchased from Sigma-Aldrich (now Merck). The surfactants were used with and without a previous purification step in order to analyze the influence of possible impurities on the mixtures. The purification was done by threefold recrystallization in acetone with traces of ethanol and was confirmed by surface tension measurements, which are presented in ESI.†

2.2 Sample preparation

The glassware which was used to prepare and store samples was cleaned with an Alconox detergent solution (Sigma-Aldrich), rinsed with ultrapure water from a Milli-Q Reference A+ purification system (18.2 MΩ cm, TOC < 5 ppb) and subsequently stored in a bath of 98% p.a. sulfuric acid (Carl Roth, Germany) with the oxidizer Nochromix (Merck) for at least 12 hours. Afterwards, the glassware was rinsed thoroughly with ultrapure water and dried in a stream of 99.999% nitrogen gas (Westfalen Gas, Germany). Stock solutions were prepared by dissolving the necessary amounts in ultrapure water including subsequent sonication for 30 minutes. All S/P mixtures were prepared by simultaneous mixing of equal volumes of surfactant and polyelectrolyte solutions with twice their intended final bulk concentration. This procedure was used in order to avoid kinetically trapped aggregates in the equilibrium one-phase region due to local concentration gradients, which are known to influence the results. More information about the latter effects and the role of different mixing protocols is provided in the work by Mezei *et al.*[19]

2.3 Electrophoretic mobility

For the determination of the electrophoretic mobility u_ζ, we used a Zetasizer Nano ZSP (Malvern, UK). All samples were measured in a backscattering geometry with the detector positioned at a scattering angle of 173°. All measurements were performed on freshly mixed samples in triplicate, and the results were averaged.

2.4 Turbidity

We performed UV/vis spectroscopy of all samples using a PerkinElmer LAMBDA 650 UV/vis spectrometer. As a measure for the turbidity of the mixtures, we evaluated the optical density (OD) at a wavelength of 450 nm since there are no specific absorption bands at this wavelength. The turbidity was measured instantly on the freshly mixed samples. After one day, four days and four weeks, the turbidity of the supernatant was measured in order to demonstrate the sedimentation behavior of the mixtures.

2.5 Surface tension

Surface tension measurements were performed with a DSA 100 (Krüss, Germany) pendant drop device. Drops were generated with a syringe at the end of a cannula with a diameter of 1.83 mm. We recorded images of the pendent drop at a rate of 1 Hz and evaluated the surface tension from the drop shape using the Young–Laplace equation. All surface tensions were evaluated after 30 minutes. It is important to keep in mind that the presented data do not represent a steady state for all samples.

The surface tension has not always reached an equilibrium value in this time scale. However, using the surface tension after 30 min is still a good measure for the surface activity of the samples and is a commonly used approach *e.g.* to establish relations between interfacial and foam properties.[4,45]

2.6 SFG spectroscopy

Sum-frequency generation (SFG) spectroscopy is an inherently interface-sensitive method that is based on the spatial and temporal overlap of two laser beams at the interface of interest. One of the impinging laser beams is a broadband femtosecond infrared (IR) pulse with the frequency ω_{IR}, while the other is a narrowband picosecond visible pulse with the frequency ω_{VIS}. A third beam with the frequency $\omega_{SF} = \omega_{IR} + \omega_{VIS}$ is generated in a second-order nonlinear optical process and detected afterwards. The intensity of the measured sum-frequency signal depends on the intensities of the two incoming laser beams and on the non-resonant and resonant second-order electric susceptibilities $\chi^{(2)}_{NR}$ and $\chi^{(2)}_{R}$, where $\chi^{(2)}_{NR}$ is mainly caused by the electronic excitations at the interface and $\chi^{(2)}_{R}$ arises due to the resonant excitation of molecular vibrations. Additional contributions from the third-order electric susceptibility $\chi^{(3)}$ are possible if a static electric field is present in the electric double layer, which originates from the adsorption of charged molecules onto an interface.[47–50] The magnitude of this contribution is a function of the Debye length κ, the wave vector mismatch Δk_z and the surface potential ϕ_0.

$$I_{SF} \propto \left|\chi^{(2)}_{NR} + \chi^{(2)}_{R} + \frac{\kappa}{\kappa + i\Delta k_z}\chi^{(3)}\phi_0\right|^2 = \left|\chi^{(2)}_{NR} + \sum_q \frac{A_q e^{i\theta}}{\omega_q - \omega_{IR} + i\Gamma_q} + \frac{\kappa}{\kappa + i\Delta k_z}\chi^{(3)}\phi_0\right|^2. \quad (1)$$

The resonant second-order susceptibility depends on the resonance frequency ω_q, the bandwidth Γ_q and the amplitude A_q of the vibrational mode q (with the phase θ), which is a function of the number of molecules at the interface and their orientational average. Without a preferred orientation of molecules, as it is the case in the bulk of centrosymmetric materials, A_q equals zero. The symmetry break at interfaces, however, causes nonzero amplitudes, and SFG spectroscopy is therefore inherently interface selective for centrosymmetric materials.

SFG spectra were recorded with a home-built spectrometer that is described elsewhere.[4,51,52] Spectra in the range of C–H and O–H vibrations (2800 to 3800 cm^{-1}) were measured by tuning the frequency of the IR beam in seven steps. The total acquisition time for the samples was between 4 and 16 minutes. All spectra presented in this study were recorded with s-polarized sum-frequency, s-polarized visible and p-polarized IR beams (ssp) and were referenced to the nonresonant SFG signal of a polycrystalline gold film that was cleaned in air plasma prior to the SFG measurement using ppp polarizations.

3. Results and discussion

3.1 Bulk behavior of NaPSS/C_nTAB mixtures

In this section, we address the behavior of C_nTAB (n = 12, 14 and 16) surfactant mixtures with sodium polystyrene sulfonate (NaPSS) in the bulk of an aqueous solution. Note that each surfactant concentration was kept constant for all measurements and was distinctly below their critical micelle concentration (CMC), which was reported to be at 0.9 mM, 3.5 mM and 15 mM for C_{16}TAB, C_{14}TAB and C_{12}TAB, respectively.[53] In fact, we have chosen for each surfactant a fixed concentration, which is ~1/6 of its respective CMC, and varied the NaPSS concentration throughout this study. The surfactant concentrations we used are summarized in Table 1.

In Fig. 1a, we present the electrophoretic mobilities of C_nTAB/NaPSS mixtures as a function of NaPSS concentration and the surfactants' chain length. The amount of surfactant bound to the NaPSS polyelectrolyte, which can be qualitatively estimated by the change in electrophoretic mobility u_ζ, is strongly dependent on the length of the surfactants' alkyl chain. In fact, this is obvious from a careful analysis of the change in u_ζ as a function of polyelectrolyte concentration in Fig. 1a. Here, in particular, an inspection of the surfactant/polyelectrolyte (S/P) mixing ratio at the point of zero net charge (PZC) where the electrophoretic mobility in the bulk vanishes is useful. Fig. 1a shows that the PZC is for C_{16}TAB at an S/P ratio of 1.3 and for C_{14}TAB at an S/P ratio of ~3.5, while with C_{12}TAB the binding is not strong enough to form charge neutral complexes (Table 1). Obviously, substantial differences in the binding of surfactants to the PSS polyelectrolyte chain exist and shift as a function of alkyl chain length. In the case of C_{16}TAB, a much more efficient binding of the surfactant is observed as the PZC is reached at close to the equal molar concentration (S/P ratio of 1.3), while in the case of C_{12}TAB, a substantial excess of the surfactant is needed to reach the PZC in the bulk. This conclusion is corroborated by previous works of Svensson *et al.* and Thalberg *et al.*[54,55] Table 1 provides a qualitative overview of the surfactants' binding efficiency. Note that all polyelectrolyte concentrations refer to the monomer concentration of NaPSS.

Because we can use the S/P ratio at the PZC as a measure of the binding efficiency of C_nTAB surfactants to PSS, it is interesting to compare the S/P ratio at the PZC for the different C_nTAB surfactants. For our further analysis of the binding properties, we make the following assumption: The charge of the polyelectrolyte is compensated by an equal charge of the surfactant, which is accomplished by a 1 : 1 binding of a

Table 1 Concentrations of apparent free and bound surfactants in the studied C_nTAB/NaPSS mixtures. PZC corresponds to the point of zero net charge in the bulk

	c_{NaPSS}/mM at PZC = $c_{surf,bound}$	$c_{surf,free}$/mM	c_{bound}/c_{total}	S/P ratio at PZC
0.1 mM C_{16}TAB	0.08	0.02	0.8	1.3
0.5 mM C_{14}TAB	0.14	0.36	0.28	3.5
2.5 mM C_{12}TAB	—	—	—	—

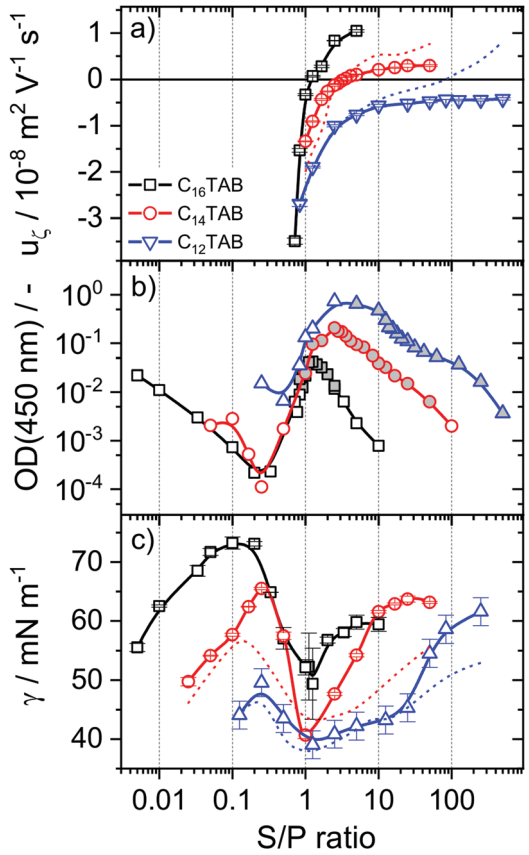

Fig. 1 Dependence of (a) the electrophoretic mobility u_ζ, (b) the optical density OD at a wavelength of 450 nm directly after mixing (additional results for extended settling times are shown in ESI†) and (c) the surface tension γ 30 min after formation of the air–water interface on the C_nTAB/NaPSS (S/P) mixing ratio (n = 12, 14, 16 as indicated in (a)). Surfactant concentrations were fixed to 0.1, 0.5 and 2.5 mM for C_{16}TAB, C_{14}TAB and C_{12}TAB, respectively, while the concentration of NaPSS was varied. Solid lines guide the eye. Dashed lines show the trends of electrophoretic mobility and surface tension of C_{12}TAB and C_{14}TAB without purification. Data points with grey filling mark the equilibrium two-phase region.

surfactant head group to a sulfonate group of the PSS chain. Following this approach, we now estimate the apparent amount of bound and free surfactants in the solution. For C_{16}TAB, about 80% of the available surfactant molecules are bound to the PSS chain at the PZC. However, at the PZC of PSS mixtures with C_{14}TAB, only 30% of the available surfactants bind to PSS, while the remainder contributes to the excess of free surfactants in the solution. For purified C_{12}TAB, the PZC cannot be reached with the chosen concentration, meaning that the binding is much weaker compared to C_{14}TAB. Here, the effect of purification can clearly be seen because C_{12}TAB, which was used as received, leads to charge neutral and even overcharged complexes. This hints at the presence of longer alkyl chains that bind stronger compared to C_{12}TAB. For the unpurified C_{14}TAB, we find the PZC at a comparable S/P ratio, meaning that the general trend is not influenced.

Mixtures of NaPSS and C_{12}TAB are well described in previous works: Ábrahám *et al.*[35] used 0.48 mM of NaPSS and found charge neutralization at a C_{12}TAB concentration of 4.8 mM (S/P = 10), while Varga *et al.*[3] showed comparable results in the same order of magnitude (6.0 mM C_{12}TAB; S/P = 12.5). While there does not seem to be a substantial effect of PSS molecular weight on this binding efficiency,[3] we found that a significantly higher S/P ratio would be necessary to reach the PZC. We have used a different approach (2.5 mM C_{12}TAB, variation of the NaPSS concentration) and cannot reach the PZC. These differences in the absolute PSS concentration hint at an additional mechanism for the higher relative surfactant concentration needed for neutralization, when the PSS concentration is low. In fact, we observe that at identical mixing ratios but different total concentrations, substantial differences in the binding of the surfactant to the polyelectrolyte exist (ESI†). This in fact explains the diverse results regarding the binding efficiency. Another possible origin for these variations are structural differences, for example a different degree of sulfonation or a different rigidity of the polyelectrolyte chain. These can arise from different synthesis routes and can have dramatic effects on the polyelectrolyte's physicochemical properties.[45,56] For instance, Abraham *et al.* discussed that the polyelectrolyte rigidity is related to its ability to wrap the surfactant aggregates and therefore strongly influences the efficiency to bind the surfactants.[36] We demonstrate the changes in u_ζ for different batches of NaPSS and as a function of S/P ratio in ESI.†

Fig. 1b presents the results of solution's turbidity as a function of S/P mixing ratio and alkyl chain length. For all three systems, we observe an equilibrium two-phase region[3] where the samples become turbid due to the formation of aggregates that cause light scattering and will eventually sediment on a long-term timescale. This region is indicated in Fig. 1b by the grey filled data points, where we define this region when the solution's optical density is decreasing after a sufficient amount of time (*e.g.* four weeks). The margins of this two-phase region were defined through long-time sedimentation experiments (more information can be found in ESI†). For mixing ratios that yield a lower mobility, the NaPSS concentration is sufficiently high to provide electrostatic stabilization due to an excess of negative charges. For low NaPSS concentrations or correspondingly for high S/P ratios, overcharged polyelectrolyte/surfactant complexes are stabilized through the excess of positive charges from the surfactants' head groups. In the case of C_{16}TAB surfactants, the concentration range of the equilibrium two-phase region is within an S/P ratio of around 0.9 and 3.5, while for C_{14}TAB, it is from S/P $\approx$ 1.25 to 50, and for C_{12}TAB surfactants, the equilibrium two-phase region starts at an S/P ratio of 3 and is continuous for higher ratios. In fact, for C_{12}TAB surfactants, no overcharging is observed, but the turbidity remains on a considerably high level even for S/P = 100. It is important to keep in mind that different surfactant concentrations were used in order to resolve the charge reversal of the polyelectrolyte/surfactant complexes for all three systems; therefore, similar S/P ratios are due to different total NaPSS concentrations for the different systems. This explains why the concentration range of the equilibrium two-phase region increases with the surfactant chain length. In the same way, we can explain the increase in optical density of the shorter surfactants.

Comparison of the optical density of the mixtures with purified and unpurified surfactants shows that the initially measured turbidity is the same for all mixtures, even for the ones with C_{12}TAB where we see significant differences in the electrophoretic mobility. However, this has consequences only for the long-term behavior of these samples. More information is shown in ESI.†

3.2 Correlation between bulk and interfacial properties

In order to relate the bulk properties of C_nTAB/NaPSS complexes to their surface activity, we have determined the surface tension of the S/P mixtures where the NaPSS concentration was varied, while the surfactant concentration was kept constant. Fig. 1c presents the surface tensions of air–water interfaces that were recorded 30 min after the air–water interfaces were created.

The changes in the surface tension of the C_{16}TAB/NaPSS mixtures are consistent with a previous report[4] on the system and demonstrate that the surface activity is highly dependent on the mixing ratio of NaPSS and C_{16}TAB. A close comparison of Fig. 1a with Fig. 1c clearly shows that at the point of zero net charge (PZC), where negligible electrophoretic mobilities (Fig. 1a) in the bulk are found, a distinct minimum in the surface tension is observed (Fig. 1c). This observation can be rationalized by a change in the hydrophobicity of charge neutral complexes or aggregates that are formed at S/P mixing ratios where the PZC in the bulk is reached. At the mixing ratios where charge neutral complexes are formed, they are more hydrophobic with a higher activity to adsorb onto air–water interfaces and thus drive the decrease in surface tension.

C_{16}TAB/NaPSS mixtures with negligible mobilities are in the equilibrium two-phase region, where sedimentation at extended waiting times is expected (see above). This is very well documented for different types of oppositely charged S/P mixtures.[3,13,34,57] Further addition of NaPSS and a reduction of the S/P ratio to a value of about 0.1 lead to a depletion of C_{16}TAB/NaPSS complexes from the air–water interface which is due to their enhanced hydrophilicity. These changes in C_{16}TAB/NaPSS mixtures with respect to the S/P ratio are consistent with those reported earlier for C_{14}TAB/poly(acrylamidomethylpropanesulfonate) (PAMPS) mixtures.[46]

From a close inspection of Fig. 1c, we conclude that the change in surface tension with S/P ratio for NaPSS mixtures with C_{14}TAB and C_{12}TAB is similar to that of C_{16}TAB, but consistent with the change in electrophoretic mobility (Fig. 1a), the excess of C_nTAB needed to reach the pronounced minimum in surface tension decreases with chain length. Although the changes in the surface tension with S/P ratio are similar for all surfactants, from Fig. 1c it is obvious that the surface tensions for surfactants with shorter alkyl chains are systematically lower ($\gamma_{C_{16}TAB} > \gamma_{C_{14}TAB} > \gamma_{C_{12}TAB}$). This can be explained by the higher concentration of both the surfactant and the polyelectrolyte and the resulting excess of free surfactants that were not bound to PSS (see Table 1 and corresponding discussion). However, surprisingly, there is a minimum in surface tension for all mixtures at an S/P ratio of 1, which we attribute to the time scale of surface tension measurements. Because the surface tensions presented in Fig. 1c were determined 30 minutes after the air–water interface was formed, the results in Fig. 1c are strongly influenced by the adsorption kinetics of free surfactants, polyelectrolytes and their complexes. In the equilibrium two-phase region, the adsorption kinetic is very slow; however, with respect to the foaming behavior and non-equilibrium properties, it is very interesting to see that equimolar mixing leads to fast kinetics. In order to understand the molecular mechanism of the latter, it is helpful to analyze the dynamic surface tension, which provides insights into the adsorption kinetics and is presented in ESI.†

Now we address the molecular order and charging state of air–water interfaces that were modified by PSS, C_nTAB and their complexes by analyzing vibrational SFG spectra (Fig. 2).

Vibrational bands which dominate the SFG spectra in Fig. 2 and their assignments to vibrational modes are summarized in Table 2.

In the following discussion of the SFG results, we concentrate first on an analysis of the C–H stretching modes (2800–3100 cm^{-1}) and later on the O–H stretching modes (3000–3800 cm^{-1}). Particularly, the ratio of the symmetric CH_2 and CH_3 stretching vibrations of the pure surfactant solutions is interesting as it provides direct information on the conformation of the surfactants' alkyl chains at the interface.[51]

While for C_{16}TAB and C_{14}TAB surfactants, no clear difference in the intensity ratio of symmetric CH_2 and CH_3 stretching vibrations at 2850 and 2878 cm^{-1} is observed, this ratio is significantly different in the SFG spectra from C_{12}TAB solutions at the air–water interface. In fact, for the air–water interfaces from the pure surfactant solutions, a small CH_2/CH_3 SFG intensity ratio (<0.1) of the symmetric stretching bands is indicative of well-ordered alkyl chains at the interface that show a low density of *gauche* conformations and a predominant all-*trans* conformation. In addition, previous studies[58–60] have shown that alkyl chain ordering is not only a function of surface coverage[58,59] but also a function of the surfactants' alkyl chain length.[60] This is because shorter chains lead to a decrease in lateral dispersive interactions and result in a lower molecular order and a higher density of *gauche* conformations. In our spectra, however, the highest molecular order was observed for C_{12}TAB surfactants. This result can be rationalized by the higher bulk concentration and consequently a higher surface excess and a more close-packed layer. This smaller CH_2/CH_3 ratio for C_{12}TAB is observed also in the mixtures for S/P ratios >25, while for low S/P ratios, the higher NaPSS concentration leads to similar CH_2/CH_3 intensity ratios for all three surfactants. Because polystyrene sulfonate also gives rise to methylene stretching bands, C–H contributions from PSS chains to the SFG spectra need to be considered in the interpretation of the SFG spectra at low S/P ratios, where complexes become the dominant species at the interface, as we will show below. In fact, this explains the close resemblance of the SFG spectra for the mixtures with low S/P ratios (Fig. 2).

While the C–H vibrations originate from both NaPSS and C_nTAB moieties at the air–water interface, the aromatic C–H stretch is a direct signature for the presence of PSS molecules at

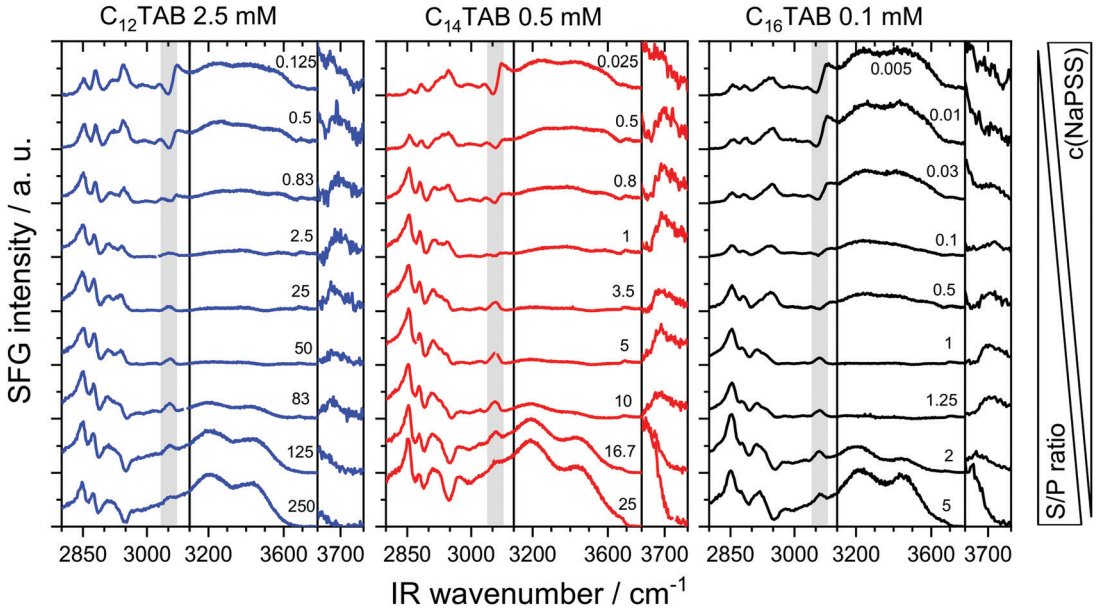

Fig. 2 Vibrational SFG spectra of C_nTAB/NaPSS modified air–water interfaces. C_nTAB/NaPSS ratios were varied as indicated next to the spectra by varying the NaPSS concentration (0 to 20 mM), while the surfactant concentrations were kept fixed to 2.5, 0.5 and 0.1 mM for C_{12}TAB, C_{14}TAB and C_{16}TAB, respectively. The spectra have an offset for better visualization. Shown is the region of C–H vibrations (aromatic C–H stretch is highlighted), the region of O–H vibrations and a close-up (10×) of the dangling O–H vibration.

Table 2 Assignments of vibrational bands

Wavenumber/cm^{-1}	Assigned molecular vibration	Ref.
2850	Methylene symmetric stretch	52, 59, 61 and 62
2878	Methyl symmetric stretch	52, 59, 61 and 62
2920	Methylene asymmetric stretch	52, 59, 61 and 62
2946	Methyl Fermi resonance	52, 59, 61 and 62
2970	Methyl asymmetric stretch	52, 59, 61 and 62
3060	Aromatic C–H stretch	52, 59, 61 and 62
3200, 3450	O–H stretch of interfacial water	52 and 63
3710	"Dangling" O–H	52 and 63

the air–water interface. Small additions of 0.05 mM NaPSS (S/P ratio ~ 5 in the case of C_{16}TAB) lead to a noticeable vibrational band at 3060 cm^{-1} (Fig. 2). In the absence of C_nTAB surfactants, the SFG spectra of solutions with a low concentration of NaPSS <2 mM were identical to the SFG spectra from the neat air–water interface without adsorbed species.[45] While the neat polyelectrolyte is not surface active at low concentrations, the increased surface activity PSS can be explained by a cooperative effect of C_nTAB surfactants and PSS polyelectrolytes and is direct evidence for the formation and adsorption of C_nTAB/PSS complexes onto the air–water interface. These complexes show obviously a higher surface activity than the neat PSS molecules, which is as expected and can be linked to the increased hydrophobicity of PSS molecules in the presence of C_nTAB surfactants.

Interestingly, S/P complexes were observed at the air–water interface for all samples when the NaPSS concentration was adjusted to >0.05 mM. From the poor surface activity of PSS (see above) and clear signatures of PSS (band at 3060 cm^{-1}) in the SFG spectra in Fig. 2, we conclude that for low S/P mixing ratios, the S/P complexes are always present at the air–water interface. This conclusion is consistent with the report by Taylor *et al.*[14] who have proposed "primary complexes" that consist of a surfactant monolayer with the polyelectrolyte backbone attached underneath. While these primary complexes are present at the surface under all circumstances, another kind of secondary complex may attach to the underside of the initial monolayer complex, which is required for stabilization of the surface and a decrease of surface tension. This description of different types of complexes is consistent with our findings especially for the NaPSS/C_{16}TAB system. Here we detect complexes at the interface with SFG at an S/P ratio of 0.1, which means that they are present at the interface, while they do not lower the surface tension compared to a neat water surface (Fig. 2c *vs.* Fig. 1c). This matches Taylor's description of "primary complexes" which do not necessarily lower the surface tension. For the two shorter surfactants, at least the trend is similar in a way that there is a local maximum at comparable S/P ratios. Higher S/P ratios lead to a lowering of the surface tension, which is consistent with the observation of secondary complexes as described by Taylor *et al.* who reported that the latter complexes tend to be more hydrophobic and adsorb onto the interface with larger surface excess. Most likely, however, this decreased surface tension around S/P ratios of 1 can be linked to the formation of aggregates. According to the results of our study, these mixing ratios lead to aggregates in the bulk (Fig. 1b); however, the physical behavior in our case is naturally different since we vary the polyelectrolyte concentration and use much higher concentrations in the mixtures. Here, aggregates that were previously formed in the bulk (Fig. 1b) are likely to be adsorbed onto the interface because of their much higher concentration. At the highest NaPSS

concentrations (lowest S/P ratio), a comparison between SFG spectra of the different C_nTAB/NaPSS mixtures reveals great similarities in terms of spectral shape and band positions. This is because at low S/P ratios there is an excess of negative charges in the mixtures (Fig. 1a). However, the absolute charge density at the air–water interface due to the presence of C_{16}TAB/PSS complexes varies between surfactants. This conclusion can be made from a close analysis of the O–H stretching bands in the SFG spectra of Fig. 2. We will now explain how conclusions about the surface charging can be made from the SFG intensity of the O–H stretching bands: eqn (1) indicates that the intensity of the SFG signal is strongly dependent on the surface potential and thus related to the surface charge *via* the Grahame equation. The probing depth, and with this the number of molecules in the near-interfacial region contributing to the SFG signal, is also a function of the Debye length and therefore the ionic strength. Since the latter two were not constant in our samples, the SFG intensity of the O–H stretching modes is partly affected by interference effects and not exclusively related to the double-layer potential according to eqn (1).[50] However, this is relevant only for ionic strengths $\ll 1$ mM, and thus care must be taken at high S/P ratios for C_{16}TAB and C_{14}TAB surfactants. In fact, for most of the concentrations, we show such effects are irrelevant and the results reflect qualitative changes in the interfacial net charge. In order to analyze the changes in the interfacial net change in more detail, we have determined the O–H intensities of the low and high frequency branches at 3200 and 3450 cm^{-1} in the SFG spectra of Fig. 2 and present the results of this analysis in Fig. 3.

From a close inspection of Fig. 3 and a comparison with Fig. 1a, it becomes obvious that the O–H intensity shows a pronounced minimum at S/P mixing ratios, where also the electrophoretic mobility in the bulk vanishes at the bulk PZC. The S/P ratio at the PZC in the bulk as shown in Table 1 is 1.3 for C_{16}TAB and 3.5 for C_{14}TAB, while there is no PZC for C_{12}TAB.

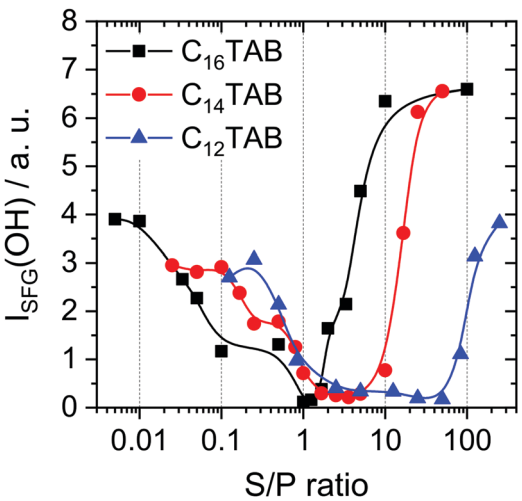

Fig. 3 Intensity of O–H vibrational bands of the measured SFG spectra as a function of the surfactant/polyelectrolyte ratio. Surfactant concentrations are 0.1 mM for C_{16}TAB, 0.5 mM for C_{14}TAB and 2.5 mM for C_{12}TAB. Solid lines guide the eye.

Mixtures with these ratios also show negligible charging at the interface, which can be deduced from negligible SFG intensities from O–H stretching bands of hydrogen-bonded interfacial water molecules. Obviously, bulk and interfacial properties in terms of electrostatics are closely related for all C_nTAB/NaPSS mixtures. Furthermore, from the results in Fig. 2 and 3, we can conclude that for mixing ratios close to the PZC, the charge neutral complexes which form aggregates in the bulk (see discussion above) dominate interfacial properties. However, we also find positively charged complexes at the interface for C_{12}TAB/PSS mixtures that show negatively charged complexes in the bulk. Compared to the behavior of the mixtures with the longer surfactants, this finding provides new insights and hints at two different types of complexes in the mixtures, one of which is negatively charged in the bulk and the other is positively charged with an excess of the surfactant and can be found at the interface.

4. Conclusions

Mixtures of oppositely charged polyelectrolyte (NaPSS) and C_nTAB surfactants with different alkyl chain lengths (n = 12, 14 and 16) have been studied in the bulk solution and at air–water interfaces. Using vibrational sum-frequency generation to study the composition and charging state of air–water interfaces and measurements of the electrophoretic mobility and the solution's turbidity, we have revealed the effects of the surfactant's chain length on their binding behavior to polystyrene sulfonate. Depending on the surfactant/polyelectrolyte (S/P) mixing ratios, we observe aggregation and phase separation in the bulk which is similar to all surfactants but at concentrations which are shifted to higher S/P ratios as the length of the alkyl chain decreases. In fact, the point of zero net charge is at S/P mixing ratios of 1.3 and 3.5 for C_{16}TAB and C_{14}TAB surfactants, while for C_{12}TAB the PZC is not crossed for the investigated concentrations. All solutions with S/P mixing ratios which showed electrophoretic mobilities within a range of -1.5 to 0.8×10^{-8} m^2 $(V\ s)^{-1}$ form complexes that are sufficiently hydrophobic to favor aggregation, which leads to turbid solutions and a long-term sedimentation of aggregates (equilibrium two-phase region). Furthermore, we can relate the phase behavior of the mixtures to the hydrophobicity and the resulting increased surface activity of S/P complexes. The margin of the equilibrium two-phase region marks a point of drastic changes within the bulk and interfacial behavior: at lower S/P ratios, complexes still carry sufficient negative charges in order to stabilize themselves against aggregation, which leads to an increase of surface tension when the S/P ratio is decreased from this point on. Higher S/P ratios however yield poorly charged complexes and aggregates that can enter the surface and lower the surface tension. Further increasing the S/P ratio leads to overcharged complexes that are again more hydrophilic and increase the surface tension. These effects lead to a minimum of the surface tension at S/P ratios of 1 for all surfactants after 30 min. This can in part be explained by the

margin of the equilibrium two-phase region, but also by the non-equilibrium state of the surface tension. In fact, the adsorption kinetics of mixtures around the PZC still show a large ongoing decrease of the surface tension, which leads to lower surface tensions when measured after a longer time, whereas for other mixing ratios, longer measurement times will not change the surface tension considerably. SFG spectroscopy shows there are complexes at the interface for all investigated mixtures, yet they do not lead to lowered surface tension in all cases. The charge of the complexes that are present at the air–water interface, as qualitatively estimated using the intensity of O–H stretching vibrations, shows excellent agreement with bulk measurements, which leads to the conclusion that aggregates formed in the bulk can enter the surface due to their hydrophobicity.

Conflicts of interest

There are no conflicts to declare.

Acknowledgements

The authors gratefully acknowledge funding from the European Research Council (ERC) under the European Union's Horizon 2020 Research and Innovation Program (Grant Agreement 638278).

References

1 S. Llamas, E. Guzmán, A. Akanno, L. Fernández-Peña, F. Ortega, R. A. Campbell, R. Miller and R. G. Rubio, Study of the Liquid/Vapor Interfacial Properties of Concentrated Polyelectrolyte–Surfactant Mixtures Using Surface Tensiometry and Neutron Reflectometry: Equilibrium, Adsorption Kinetics, and Dilational Rheology, *J. Phys. Chem. C*, 2018, **122**, 4419–4427, DOI: 10.1021/acs.jpcc.7b12457.

2 S. Llamas, L. Fernández-Peña, A. Akanno, E. Guzmán, V. Ortega, F. Ortega, A. G. Csaky, R. A. Campbell and R. G. Rubio, Towards understanding the behavior of polyelectrolyte–surfactant mixtures at the water/vapor interface closer to technologically-relevant conditions, *Phys. Chem. Chem. Phys.*, 2018, **20**, 1395–1407, DOI: 10.1039/c7cp05528e.

3 I. Varga and R. A. Campbell, General Physical Description of the Behavior of Oppositely Charged Polyelectrolyte/Surfactant Mixtures at the Air/Water Interface, *Langmuir*, 2017, **33**, 5915–5924, DOI: 10.1021/acs.langmuir.7b01288.

4 F. Schulze-Zachau and B. Braunschweig, Structure of Polystyrenesulfonate/Surfactant Mixtures at Air–Water Interfaces and Their Role as Building Blocks for Macroscopic Foam, *Langmuir*, 2017, **33**, 3499–3508, DOI: 10.1021/acs.langmuir.7b00400.

5 L. Piculell and B. Lindman, Association and segregation in aqueous polymer/polymer, polymer/surfactant, and surfactant/surfactant mixtures: similarities and differences, *Adv. Colloid Interface Sci.*, 1992, **41**, 149–178, DOI: 10.1016/0001-8686(92)80011-L.

6 S. Llamas, E. Guzmán, F. Ortega, N. Baghdadli, C. Cazeneuve, R. G. Rubio and G. S. Luengo, Adsorption of polyelectrolytes and polyelectrolytes–surfactant mixtures at surfaces: a physico-chemical approach to a cosmetic challenge, *Adv. Colloid Interface Sci.*, 2015, **222**, 461–487, DOI: 10.1016/j.cis.2014.05.007.

7 E. D. Goddard, Polymer/Surfactant Interaction: Interfacial Aspects, *J. Colloid Interface Sci.*, 2002, **256**, 228–235, DOI: 10.1006/jcis.2001.8066.

8 C. D. Bain, P. M. Claesson, D. Langevin, R. Meszaros, T. Nylander, C. Stubenrauch, S. Titmuss and R. von Klitzing, Complexes of surfactants with oppositely charged polymers at surfaces and in bulk, *Adv. Colloid Interface Sci.*, 2010, **155**, 32–49, DOI: 10.1016/j.cis.2010.01.007.

9 E. Guzmán, S. Llamas, A. Maestro, L. Fernández-Peña, A. Akanno, R. Miller, F. Ortega and R. G. Rubio, Polymer–surfactant systems in bulk and at fluid interfaces, *Adv. Colloid Interface Sci.*, 2016, **233**, 38–64, DOI: 10.1016/j.cis.2015.11.001.

10 K. Szczepanowicz, U. Bazylińska, J. Pietkiewicz, L. Szyk-Warszyńska, K. A. Wilk and P. Warszyński, Biocompatible long-sustained release oil-core polyelectrolyte nanocarriers: from controlling physical state and stability to biological impact, *Adv. Colloid Interface Sci.*, 2015, **222**, 678–691, DOI: 10.1016/j.cis.2014.10.005.

11 P. Hössel, R. Dieing, R. Nörenberg, A. Pfau and R. Sander, Conditioning polymers in today's shampoo formulations – efficacy, mechanism and test methods, *Int. J. Cosmet. Sci.*, 2000, **22**, 1–10, DOI: 10.1046/j.1467-2494.2000.00003.x.

12 *Polymer–surfactant systems*, ed. J. C. T. Kwak, Dekker, New York, NY, 1998, vol. 77.

13 A. Akanno, E. Guzmán, L. Fernández-Peña, S. Llamas, F. Ortega and R. G. Rubio, Equilibration of a Polycation-Anionic Surfactant Mixture at the Water/Vapor Interface, *Langmuir*, 2018, **34**, 7455–7464, DOI: 10.1021/acs.langmuir.8b01343.

14 D. J. F. Taylor, R. K. Thomas, P. X. Li and J. Penfold, Adsorption of Oppositely Charged Polyelectrolyte/Surfactant Mixtures. Neutron Reflection from Alkyl Trimethylammonium Bromides and Sodium Poly(styrenesulfonate) at the Air/Water Interface: The Effect of Surfactant Chain Length, *Langmuir*, 2003, **19**, 3712–3719, DOI: 10.1021/la020709e.

15 D. J. F. Taylor, R. K. Thomas and J. Penfold, The Adsorption of Oppositely Charged Polyelectrolyte/Surfactant Mixtures: Neutron Reflection from Dodecyl Trimethylammonium Bromide and Sodium Poly(styrene sulfonate) at the Air/Water Interface, *Langmuir*, 2002, **18**, 4748–4757, DOI: 10.1021/la011716q.

16 J. Penfold, I. Tucker, R. K. Thomas, D. J. F. Taylor, J. Zhang and X. L. Zhang, The impact of electrolyte on the adsorption of sodium dodecyl sulfate/polyethyleneimine complexes at the air-solution interface, *Langmuir*, 2007, **23**, 3690–3698, DOI: 10.1021/la063017p.

17 R. A. Campbell, A. Tummino, B. A. Noskov and I. Varga, Polyelectrolyte/surfactant films spread from neutral aggregates, *Soft Matter*, 2016, **12**, 5304–5312, DOI: 10.1039/c6sm00637j.

18 A. Tummino, J. Toscano, F. Sebastiani, B. A. Noskov, I. Varga and R. A. Campbell, Effects of Aggregate Charge

and Subphase Ionic Strength on the Properties of Spread Polyelectrolyte/Surfactant Films at the Air/Water Interface under Static and Dynamic Conditions, *Langmuir*, 2018, **34**, 2312–2323, DOI: 10.1021/acs.langmuir.7b03960.

19 A. Mezei, R. Meszaros, I. Varga and T. Gilanyi, Effect of mixing on the formation of complexes of hyperbranched cationic polyelectrolytes and anionic surfactants, *Langmuir*, 2007, **23**, 4237–4247, DOI: 10.1021/la0635294.

20 J. L. Ortega-Vinuesa, A. Martín-Rodríguez and R. Hidalgo-Álvarez, Colloidal Stability of Polymer Colloids with Different Interfacial Properties: Mechanisms, *J. Colloid Interface Sci.*, 1996, **184**, 259–267, DOI: 10.1006/jcis.1996.0619.

21 Q. Deng, H. Li, C. Li, W. Lv and Y. Li, Enhancement of foamability and foam stability induced by interactions between a hyperbranched exopolysaccharide and a zwitterionic surfactant dodecyl sulfobetaine, *RSC Adv.*, 2015, **5**, 61868–61875, DOI: 10.1039/c5ra09120a.

22 A. Aziz, H. C. Hailes, J. M. Ward and J. R. G. Evans, Long-term stabilization of reflective foams in sea water, *RSC Adv.*, 2014, **4**, 53028–53036, DOI: 10.1039/C4RA08714C.

23 N. Kristen-Hochrein, A. Laschewsky, R. Miller and R. Klitzing, Stability of foam films of oppositely charged polyelectrolyte/surfactant mixtures: effect of isoelectric point, *J. Phys. Chem. B*, 2011, **115**, 14475–14483, DOI: 10.1021/jp206964k.

24 S. B. Aidarova, K. B. Musabekov, Z. B. Ospanova and M. Guden, Foaming binary solution mixtures of low molecular surfactant and polyelectrolyte, *J. Mater. Sci.*, 2006, **41**, 3979–3986, DOI: 10.1007/s10853-006-7573-9.

25 J. F. Argillier, S. Zeilinger and P. Roche, Enhancement of Aqueous Emulsion and Foam Stability with Oppositely Charged Surfactant/Polyelectrolyte Mixed Systems, *Oil Gas Sci. Technol.*, 2009, **64**, 597–605, DOI: 10.2516/ogst/2009043.

26 M. Uhlig, R. Miller and R. Klitzing, Surface adsorption of sulfonated poly(phenylene sulfone)/C14TAB mixtures and its correlation with foam film stability, *Phys. Chem. Chem. Phys.*, 2016, **18**, 18414–18423, DOI: 10.1039/c6cp02256a.

27 C. Monteux, G. Fuller and V. Bergeron, Shear and Dilational Surface Rheology of Oppositely Charged Polyelectrolyte/Surfactant Microgels Adsorbed at the Air–Water Interface. Influence on Foam Stability, *J. Phys. Chem. B*, 2004, **108**, 16473–16482, DOI: 10.1021/jp047462.

28 C. Monteux, C. E. Williams, J. Meunier, O. Anthony and V. Bergeron, Adsorption of Oppositely Charged Polyelectrolyte/Surfactant Complexes at the Air/Water Interface, *Langmuir*, 2004, **20**, 57–63, DOI: 10.1021/la0347861.

29 H. Ritacco, P.-A. Albouy, A. Bhattacharyya and D. Langevin, Influence of the polymer backbone rigidity on polyelectrolyte–surfactant complexes at the air/water interface, *Phys. Chem. Chem. Phys.*, 2000, **2**, 5243–5251, DOI: 10.1039/b004657o.

30 M. Gradzielski and I. Hoffmann, Polyelectrolyte–surfactant complexes (PESCs) composed of oppositely charged components, *Curr. Opin. Colloid Interface Sci.*, 2018, **35**, 124–141, DOI: 10.1016/j.cocis.2018.01.017.

31 I. Hoffmann, P. Heunemann, S. Prévost, R. Schweins, N. J. Wagner and M. Gradzielski, Self-aggregation of mixtures of oppositely charged polyelectrolytes and surfactants studied by rheology, dynamic light scattering and small-angle neutron scattering, *Langmuir*, 2011, **27**, 4386–4396, DOI: 10.1021/la104588b.

32 B. K. Schabes, R. M. Altman and G. L. Richmond, Come Together: Molecular Details into the Synergistic Effects of Polymer–Surfactant Adsorption at the Oil/Water Interface, *J. Phys. Chem. B*, 2018, **122**, 8582–8590, DOI: 10.1021/acs.jpcb.8b05432.

33 K. Bali, Z. J. Varga, A. Kardos, I. Varga, T. Gilányi, A. Domján, A. Wacha, A. Bóta, J. Mihály and R. Mészáros, Effect of Dilution on the Nonequilibrium Polyelectrolyte/Surfactant Association, *Langmuir*, 2018, **34**, 14652–14660, DOI: 10.1021/acs.langmuir.8b03255.

34 R. A. Campbell, A. Angus-Smyth, M. Yanez Arteta, K. Tonigold, T. Nylander and I. Varga, New Perspective on the Cliff Edge Peak in the Surface Tension of Oppositely Charged Polyelectrolyte/Surfactant Mixtures, *J. Phys. Chem. Lett.*, 2010, **1**, 3021–3026, DOI: 10.1021/jz101179f.

35 Á. Ábrahám, A. Kardos, A. Mezei, R. A. Campbell and I. Varga, Effects of ionic strength on the surface tension and nonequilibrium interfacial characteristics of poly(sodium styrenesulfonate)/dodecyltrimethylammonium bromide mixtures, *Langmuir*, 2014, **30**, 4970–4979, DOI: 10.1021/la500637v.

36 Á. Ábrahám, R. A. Campbell and I. Varga, New method to predict the surface tension of complex synthetic and biological polyelectrolyte/surfactant mixtures, *Langmuir*, 2013, **29**, 11554–11559, DOI: 10.1021/la402525w.

37 B. A. Noskov, G. Loglio and R. Miller, Dilational Viscoelasticity of Polyelectolyte/Surfactant Adsorption Films at the Air/Water Interface: Dodecyltrimethylammonium Bromide and Sodium Poly(styrenesulfonate), *J. Phys. Chem. B*, 2004, **108**, 18615–18622, DOI: 10.1021/jp046560s.

38 B. A. Noskov, G. Loglio and R. Miller, Dilational surface viscoelasticity of polyelectrolyte/surfactant solutions: formation of heterogeneous adsorption layers, *Adv. Colloid Interface Sci.*, 2011, **168**, 179–197, DOI: 10.1016/j.cis.2011.02.010.

39 J. Penfold, R. K. Thomas and D. J. F. Taylor, Polyelectrolyte/surfactant mixtures at the air–solution interface, *Curr. Opin. Colloid Interface Sci.*, 2006, **11**, 337–344, DOI: 10.1016/j.cocis.2006.08.003.

40 T. Vongsetskul, D. J. F. Taylor, J. Zhang, P. X. Li, R. K. Thomas and J. Penfold, Interaction of a cationic gemini surfactant with DNA and with sodium poly(styrene sulphonate) at the air/water interface: a neutron reflectometry study, *Langmuir*, 2009, **25**, 4027–4035, DOI: 10.1021/la802816s.

41 R. A. Campbell, P. A. Ash and C. D. Bain, Dynamics of adsorption of an oppositely charged polymer–surfactant mixture at the air–water interface: poly(dimethyldiallylammonium chloride) and sodium dodecyl sulfate, *Langmuir*, 2007, **23**, 3242–3253, DOI: 10.1021/la0632171.

42 A. Angus-Smyth, C. D. Bain, I. Varga and R. A. Campbell, Effects of bulk aggregation on PEI–SDS monolayers at the dynamic air–liquid interface, *Soft Matter*, 2013, **9**, 6103, DOI: 10.1039/c3sm50636c.

43 A. Angus-Smyth, R. A. Campbell and C. D. Bain, Dynamic adsorption of weakly interacting polymer/surfactant

mixtures at the air/water interface, *Langmuir*, 2012, **28**, 12479–12492, DOI: 10.1021/la301297s.

44 O. Y. Milyaeva, R. A. Campbell, S.-Y. Lin, G. Loglio, R. Miller, M. M. Tihonov, I. Varga, A. V. Volkova and B. A. Noskov, Synergetic effect of sodium polystyrene sulfonate and guanidine hydrochloride on the surface properties of lysozyme solutions, *RSC Adv.*, 2015, **5**, 7413–7422, DOI: 10.1039/C4RA14330B.

45 F. Schulze-Zachau, S. Bachmann and B. Braunschweig, Effects of Ca^{2+} Ion Condensation on the Molecular Structure of Polystyrene Sulfonate at Air–Water Interfaces, *Langmuir*, 2018, **34**, 11714–11722, DOI: 10.1021/acs.langmuir.8b02631.

46 H. Fauser, R. Klitzing and R. A. Campbell, Surface adsorption of oppositely charged C14TAB-PAMPS mixtures at the air/water interface and the impact on foam film stability, *J. Phys. Chem. B*, 2015, **119**, 348–358, DOI: 10.1021/jp509631b.

47 G. Gonella and C. Lütgebaucks, de Beer, Alex G. F. and S. Roke, Second Harmonic and Sum-Frequency Generation from Aqueous Interfaces Is Modulated by Interference, *J. Phys. Chem. C*, 2016, **120**, 9165–9173, DOI: 10.1021/acs.jpcc.5b12453.

48 P. E. Ohno, H.-F. Wang and F. M. Geiger, Second-order spectral lineshapes from charged interfaces, *Nat. Commun.*, 2017, **8**, 203, DOI: 10.1038/s41467-017-01088-0.

49 P. E. Ohno, S. A. Saslow, H.-F. Wang, F. M. Geiger and K. B. Eisenthal, Phase-referenced nonlinear spectroscopy of the α-quartz/water interface, *Nat. Commun.*, 2016, **7**, 13587, DOI: 10.1038/ncomms13587.

50 J. Schaefer, G. Gonella and M. Bonn, and Backus, Ellen H. G., Surface-specific vibrational spectroscopy of the water/silica interface: screening and interference, *Phys. Chem. Chem. Phys.*, 2017, **19**, 16875–16880, DOI: 10.1039/c7cp02251d.

51 C. Meltzer, J. Paul, H. Dietrich, C. M. Jäger, T. Clark, D. Zahn, B. Braunschweig and W. Peukert, Indentation and self-healing mechanisms of a self-assembled monolayer – a combined experimental and modeling study, *J. Am. Chem. Soc.*, 2014, **136**, 10718–10727, DOI: 10.1021/ja5048076.

52 K. Engelhardt, W. Peukert and B. Braunschweig, Vibrational sum-frequency generation at protein modified air–water interfaces: effects of molecular structure and surface charging, *Curr. Opin. Colloid Interface Sci.*, 2014, **19**, 207–215, DOI: 10.1016/j.cocis.2014.03.008.

53 C. Stubenrauch and K. Khristov, Foams and foam films stabilized by C_nTAB: influence of the chain length and of impurities, *J. Colloid Interface Sci.*, 2005, **286**, 710–718, DOI: 10.1016/j.jcis.2005.01.107.

54 A. Svensson, J. Norrman and L. Piculell, Phase behavior of polyion–surfactant ion complex salts: effects of surfactant chain length and polyion length, *J. Phys. Chem. B*, 2006, **110**, 10332–10340, DOI: 10.1021/jp057402j.

55 K. Thalberg, B. Lindman and G. Karlstroem, Phase behavior of systems of cationic surfactant and anionic polyelectrolyte: influence of surfactant chain length and polyelectrolyte molecular weight, *J. Phys. Chem.*, 1991, **95**, 3370–3376, DOI: 10.1021/j100161a073.

56 A. K. Sen, S. Roy and V. A. Juvekar, Effect of structure on solution and interfacial properties of sodium polystyrene sulfonate (NaPSS), *Polym. Int.*, 2007, **56**, 167–174, DOI: 10.1002/pi.2154.

57 R. A. Campbell, M. Yanez Arteta, A. Angus-Smyth, T. Nylander, B. A. Noskov and I. Varga, Direct impact of nonequilibrium aggregates on the structure and morphology of Pdadmac/SDS layers at the air/water interface, *Langmuir*, 2014, **30**, 8664–8674, DOI: 10.1021/la500621t.

58 C. Meltzer, H. Dietrich, D. Zahn, W. Peukert and B. Braunschweig, Self-Assembled Monolayers Get Their Final Finish *via* a Quasi-Langmuir–Blodgett Transfer, *Langmuir*, 2015, **31**, 4678–4685, DOI: 10.1021/acs.langmuir.5b00440.

59 C. Meltzer, H. Yu, W. Peukert and B. Braunschweig, Molecular structure of octadecylphosphonic acids during their self-assembly on α-Al_2O_3(0001), *Phys. Chem. Chem. Phys.*, 2018, **20**, 19382–19389, DOI: 10.1039/C8CP02391C.

60 A. Pathak, A. Bora, B. Braunschweig, C. Meltzer, H. Yan, P. Lemmens, W. Daum, J. Schwartz and M. Tornow, Nanocylindrical confinement imparts highest structural order in molecular self-assembly of organophosphonates on aluminum oxide, *Nanoscale*, 2017, **9**, 6291–6295, DOI: 10.1039/C7NR02420G.

61 K. Engelhardt, U. Weichsel, E. Kraft, D. Segets, W. Peukert and B. Braunschweig, Mixed layers of β-lactoglobulin and SDS at air–water interfaces with tunable intermolecular interactions, *J. Phys. Chem. B*, 2014, **118**, 4098–4105, DOI: 10.1021/jp501541q.

62 A. Ge, M. Matsusaki, L. Qiao, M. Akashi and S. Ye, Salt Effects on Surface Structures of Polyelectrolyte Multilayers (PEMs) Investigated by Vibrational Sum Frequency Generation (SFG) Spectroscopy, *Langmuir*, 2016, **32**, 3803–3810, DOI: 10.1021/acs.langmuir.5b04765.

63 Y. R. Shen and V. Ostroverkhov, Sum-frequency vibrational spectroscopy on water interfaces: polar orientation of water molecules at interfaces, *Chem. Rev.*, 2006, **106**, 1140–1154, DOI: 10.1021/cr040377d.